Am J Clin Exp Urol 2026;14(1):34-44
www.ajceu.us /ISSN:2330-1910/AJCEU0169107

Original Article

Peripheral serotonin contributes to testosterone and estradiol induced urinary voiding dysfunction in adult male mice

Jojo Maier[1,2*], Elliot Heye[3*], Monica Ridlon[3], Marcela Ambrogi[3], Douglas W Strand[4], Kimberly P Keil-Stietz[3], Chad M Vezina[3]

[1]Department of Medicine, Division of Endocrinology, Diabetes, and Metabolism University of Wisconsin-Madison, Madison, WI 537063, United States; [2]Research Service, William S. Middleton Memorial Veterans Hospital, Madison, WI 53705, United States; [3]Department of Comparative Biosciences, University of Wisconsin-Madison, Madison, WI 53706, United States; [4]Department of Urology, UT Southwestern Medical Center, Dallas, TX 75390, United States. [*]Equal contributors.

Received September 30, 2025; Accepted February 12, 2026; Epub February 15, 2026; Published February 28, 2026

Abstract: Objective: Millions of aging men are diagnosed with lower urinary tract dysfunction (LUTD) each year. Alpha adrenergic receptor blockers relax prostatic, urethral, and bladder smooth muscle to relieve LUTD symptoms and are often, but not always, effective. Serotonin is proposed to cause contractions in the female urethra, as well as in the lungs and bowel. This study tests that serotonin synthesized in the periphery, outside of the central nervous system, contributes to the development of LUTD induced in mice by subcutaneous implants of testosterone (T) and estradiol (E2), mimicking the hormone milieu of aging men. Methods: Immunofluorescent staining of male human and mouse urethra was used to confirm the presence of neuroendocrine cells and interstitial cells of Cajal, which contribute to serotonin-induced contractions in the female mouse urethra. Wild type and tryptophan hydroxylase 1 null (*Tph1*$^{-/-}$) mice, which are deficient in the rate-limiting enzyme in peripheral serotonin synthesis, were given sham surgery or T+E2 implants. Voiding behavior was measured with the void spot assay one day before surgery and two weeks post-surgery. Four weeks after surgery, bladders were exteriorized and measured to calculate volume, and anesthetized cystometry was performed to assess bladder activity. Results: Serotonin-positive neuroendocrine cells and serotonin receptor positive interstitial cells of Cajal were detected in the prostatic urethra of humans and mice. Two weeks after T+E2 implantation surgery, a baseline level of urinary retention occurred in both wild type and *Tph1*$^{-/-}$ mice. However, wild type mice treated with T+E2 had increased frequent small voids ($P<0.01$) and decreased bladder activity ($P<0.005$) when compared to wild type mice with sham treatment and *Tph1*$^{-/-}$ mice with T+E2 treatment. Conclusions: Wild type mice developed a more severe voiding dysfunction phenotype than *Tph1*$^{-/-}$ mice when treated with T+E2, indicating that peripheral serotonin plays a role in T+E2-mediated LUTD. Because the urinary dysfunction observed in mice mimics that of human men, future studies to understand and exploit the role of serotonin may provide a treatment option for a subset of LUTD.

Keywords: Serotonin, Serotonin receptor 2B (5HTR2B), neuroendocrine cells, interstitial cells of Cajal (ICC), lower urinary tract symptoms (LUTS), lower urinary tract dysfunction (LUTD), urology, translational animal models

Introduction

Lower urinary tract dysfunction (LUTD) affects millions of aging men and can trigger tract symptoms (LUTS) that may include weak urinary stream, incomplete bladder emptying, and nocturia [1, 2]. While treatments such as alpha-adrenergic blockers and 5 alpha reductase inhibitors can be effective, the complex nature of the disease complicates treatment. LUTD etiology is multifactorial and has been linked to exposure to environmental toxins [3-5], chronic prostate inflammation [6, 7], benign prostatic hyperplasia (BPH), and increased smooth muscle tone [8, 9]. An aging-related reduction in the ratio of circulating testosterone to 17β estradiol is also hypothesized to contribute to LUTD in men [10-12]. Administration of exogenous tes-

https://doi.org/10.62347/QDWM4583

tosterone and estradiol (T+E2) to male mice [13-15], rats [16, 17], and dogs [11, 18], to simulate age-related hormonal imbalances, elicits a pattern of voiding dysfunction that resembles features of LUTD in aging men, which includes frequent, low volume voids [14, 15], urinary retention in the bladder [13, 17, 19], and hydronephrosis [15]. At the molecular and cellular levels, treatment with exogenous T+E2 in male rodents and dogs leads to prostatic epithelium and stroma proliferation [11, 15, 20, 21], low grade inflammation [17, 22, 23], bladder contractile deficiencies [16, 24], thickening of bladder smooth muscle [14, 25], and modulation of adrenoreceptor, anoctamin 1 (ANO1), and sex steroid receptor responsiveness [26-28]. However, the full mechanism by which exogenous T+E2 drives urinary dysfunction, especially in the urethra, is not known.

We recently described a smooth muscle mediated defense mechanism in the female mouse urethra that protects the host from invading uropathogens [29]. Uropathogens stimulate serotonin release from urethral neuroendocrine cells, activating urethral pacemaker cells (interstitial cells of Cajal, ICC) that act via ANO1 receptors [28, 30], driving urethral smooth muscle contractions to expel bacteria [29]. Contractions in the prostatic urethra have been linked to male LUTS and are treated with alpha blockers, but some men remain symptomatic. The purpose of this study was to test whether cells mediating female urethral serotonin signaling are also present in male urethra, and to determine whether non-neuronal serotonin, including serotonin produced by urethral neuroendocrine cells, is required for T+E2-induced voiding dysfunction in adult male mice.

We used immunofluorescent staining to confirm the presence of serotonin-synthesizing neuroendocrine cells and serotonin-receptor-positive interstitial cells of Cajal in the human and male mouse prostatic urethra, confirming the cross-sex relevance of the previous female based studies [29]. We also tested if peripheral serotonin is required for the development of T+E2-induced voiding dysfunction by comparing wild type control C57BL/6J mice to mice lacking tryptophan hydroxylase 1 (*Tph1*$^{-/-}$), which catalyzes the rate limiting step in serotonin production outside of the central nervous system. Wild type and *Tph1*$^{-/-}$ mice were given sham surgeries or given slow-release subcutaneous T and E2 implants in the scapular fat pad. We assessed voiding behavior, urine-filled bladder volume, and bladder functionality in wild type and *Tph1*$^{-/-}$ mice treated with sham and T+E2 pellets. Peripheral serotonin was required for some T+E2 driven urinary endpoints, including increased void spot number and total voided volume, and loss of bladder contractility as assessed by cystometry, suggesting that peripheral serotonin is in part required for T+E2-mediated voiding dysfunction.

Material and methods

Mice

All experiments were conducted in strict adherence to the approved protocol from the University of Wisconsin-Madison Animal Care and Use Committee (ID: V005096), following the guidelines outlined in the National Institutes of Health Guide for the Care and Use of Laboratory Animals. Mice were housed in Udel Polysulfone microisolator cages on racks or in Innocage disposable mouse cages on an Innorack (Innovive, San Diego, CA). Room lighting was maintained on a 12:12-h light-dark cycles, room temperature was maintained at 20.5±5°C, and humidity was 30-70%. Mice were fed no. 8604 Teklad Rodent Diet (Harlan Laboratories, Madison, WI), and feed and water were available ad libitum. Cages contained corn cob bedding. Mice were euthanized via CO_2 asphyxiation with CO_2 introduced to the chamber at 3 liters/min. Clinical death was confirmed with cervical dislocation.

Hormone capsule preparation and implantation

Eight-week-old C57BL/6J and *Tph1*$^{-/-}$ male mice were anesthetized with isoflurane, and compressed pellets of 25 mg T, 2.5 mg E2, and 22.5 mg cholesterol were implanted subcutaneously into the scapular fat pad (control mice received sham surgeries) as previously described [14, 15]. The pellets disintegrate and dissolve slowly over time to release hormones into the subcutaneous space, which is subsequently absorbed into systemic circulation. Mice were euthanized between 12 and 14 weeks of age. Experimental group sizes for all mouse experiments are detailed in **Table 1**.

Table 1. Experimental group size (N values) for all mouse experiments

N values	Wild Type		*Tph1*$^{-/-}$	
	Sham	T+E2	Sham	T+E2
Total Implanted	12	12	10	10
Void Spot Assay	5	6	6	4
Cystometry and Bladder Volumetrics	6	7	5	6

Table 2. Demographic information for human tissue samples used in **Figure 1**

Human Prostate Specimens			
Donor ID	Age	Ethnicity	Figure
D21	58	White	1B
D32	24	Black	1A, 1C
BPH ID	Age	Ethnicity	Figure
BPH 239	78	Hispanic/Latino	1A
BPH 247	Unknown	Unknown	1A, 1B
BPH 249	Unknown	Unknown	1B
BPH 265	66	White	1C
BPH 274	75	White	1C

Sample sizes were modeled off previous studies that utilized the T+E2 model [15, 24, 25].

Mouse prostate

Complete lower urinary tracts of wild type male mice, distinct from those used in the mouse experiments described in this study, were embedded into paraffin blocks and sectioned for immunolabeling as previously described [31-33].

Human prostate

Donor prostates were collected by cystoprostatectomy, after the collection of transplantable organs, at the Southwest Transplant Alliance under Institutional Review Board STU 112014-033. Donor families provided written consent allowing the use of prostate tissues for research studies in accordance with UTSW IRB. Prostate specimens from patients seeking treatment for LUTD were collected by simple prostatectomy at UTSW and are referred to as "BPH" samples. All samples were deidentified prior to distribution, and known demographic information is detailed in **Table 2**. Tissue samples were transported in ice-cold saline and dissected into portions for fixation in 10% formalin followed by paraffin embedding. Blocks were then cut into five-micron sections.

Immunofluorescent staining

Five-micron male mouse and human tissue sections were deparaffinized with xylenes and rehydrated through a series of ethanol dilutions. Tissue sections were then submerged in a 6.0 pH citrate buffer and heated for 20 minutes in a microwave to decloak epitopes. Tris-buffered saline containing 0.1% Tween 20 and 5% donkey serum was used as a blocking reagent, and primary and secondary antibodies were diluted in blocking reagent. Primary antibodies and dilutions used were: mouse anti-e-cadherin (CDH1, BD Transduction Labs, catalog #610182, 1:250), rabbit anti-ANO1 (Abcam, catalog #AB64084, 1:100), mouse anti-serotonin receptor 2B (HTR2B, Santa Cruz, catalog #SC-376878, 1:200), rat anti-serotonin (EMD Millipore, catalog #MAB352, 1:50), mouse anti-smooth muscle actin alpha (ACTA2, Leica, catalog #ncl-sma, 1:250), rabbit anti-synaptophysin (SYP, Invitrogen, catalog #MA5-14532, 1:200). Secondary antibodies and dilutions used were: donkey anti-mouse Alexa 488 (Jackson ImmunoResearch, catalog #715-545-150, 1:250), donkey anti-rabbit rhodamine red™-X (RRX) (Jackson ImmunoResearch, catalog #711-295-152, 1:250), donkey anti-rat Alexa 647 (Jackson ImmunoResearch, catalog #712-605-153, 1:250), and donkey anti-mouse Alexa 647 (Jackson ImmunoResearch, catalog #715-605-150, 1:250). Antibodies were previously utilized for cell identification in the female urethra [29], have been validated in knockout tissue [34], and used in LUT cell identification [35]. Tissue sections were imaged using an Eclipse E600 compound microscope (Nikon Instruments Inc., Melville, NY) fitted with a 20x dry objective (Plan Fluor NA = 0.75; Nikon, Melville, NY) and equipped with NIS elements imaging software (Nikon Instruments Inc.). Fluorescence was detected using DAPI (2-(4-amidinophenyl)-1H-indole-6-carboxamidine), FITC, Texas Red (Chroma Technology Corp, Bellows Fall, VT), and CY5 filter cubes (Nikon, Melville, NY).

Void spot assay

All guidelines for reporting and performing void spot assay (VSA) were followed [36]. Wild type

and *Tph1*$^{-/-}$ mice were introduced to singly housed caging that was equivalent to their normal housing, with ad libitum food access but no access to water. The bottom of the cage was fitted with Whatman grade 540 (Fisher Scientific no. 057163-W) filter papers (27×16 cm). All testing was conducted in the same quiet location and at the same time of day. Mice were tested in the experimental housing for four hours and then returned to their home cage. This experiment was conducted before the implantation surgery to establish a baseline for each treatment group, and then again two weeks after the implantation.

Filter papers were imaged with an Autochemi AC1 Darkroom ultraviolet imaging cabinet (UVP, Upland, CA) equipped with an Auto Chemi Zoom lens 2UV and an epi-illuminator. Image capture settings were adjusted using UVP VisonWorksLS image acquisition software. Images were captured using an Ethidium Bromide filter set (570-640 nm) and 365 nm epi-illumination. Exposure settings were optimized to maximize signal over noise. Images were then analyzed with VoidWhizzard, a plugin for FIJI imageJ created to analyze void spot data [38]. Analyzed parameters included: total spot count, total void area (in cm^2), percent area in the center of the paper, percent area in the corners of the paper, and mass distribution of spots (0-0.1, 0.1-0.25, 0.25-0.5, 0.5-1, 1-2, 2-3, 3-4, and 4+ cm).

Cystometry

Cystometry was performed as previously described [24, 38]. Mice were first anesthetized with urethane with a weight dependent dosing paradigm (1.43 mg/g for 0-25 g mouse, 1.4 mg/g for 25-35 g mouse, and 1.2 mg/g for >35 g mouse). An incision in the abdominal wall was used to expose the bladder. Bladder volume was estimated through three orthogonal measurements using calipers. A purse string suture was created around the apex of the bladder. PE-50 tubing was cut to approximately 35 mm and placed on a 1.5-in., 26-gauge syringe needle, and one end of the tubing was melted to create a cuff. The needle and tubing were inserted through the apex of the bladder. After removing the needle, the purse string sutures were tightened, and two circumferential sutures were added to secure the catheter. The incision was sutured, and mice were given 45 minutes to recover on a heated pad.

The catheter was connected to a three-way stopcock, which was then attached to an infusion pump and pressure transducer. Mouse bladders were infused with saline through the catheter at a rate of 0.8 mL/hour. Bladder pressure was continuously recorded using a PowerLab data collection system (AD Instruments, Dunedin, New Zealand). Voiding was recorded for at least 1 hour. Additional measures obtained from cystometry were not analyzed due to insufficient complete voids.

Statistics

Statistical analysis was performed using R 4.4.3 and R Studio 2024.12.1. Generally, data was tested for normality using a Shapiro-Wilkes test. If needed, a Boxcox test was used to identify an appropriate transformation to achieve normality. Transformations are described in figure legends. A two-way ANOVA was used to analyze normal and transformed data, followed by a post-hoc Tukey's multiple comparisons test. Categorical or binary data was analyzed with the Fisher's exact test. The raw data is shown in all figures. A *p*-value of less than 0.05 was considered statistically significant in all analyses.

Results

The mouse and human prostatic urethra contain serotonin expressing neuroendocrine cells and serotonin receptor expressing interstitial cells of Cajal

We used immunofluorescent staining to test for the presence of male prostatic urethral cells that resemble cells identified to mediate serotonin-induced urethral contraction in the female [29]. We observed rare synaptophysin, serotonin, and e-cadherin triple positive cells, characteristic of neuroendocrine cells [39, 40], in male mouse and human prostatic urethra (**Figure 1A**). In female urethras, serotonin binding to 5-HTR on ICCs begins an action potential in the surrounding smooth muscle [29]. We confirmed the presence of elongated ANO1 cells that were embedded within ACTA2-positive smooth muscle of mouse and human prostatic urethra (**Figure 1B**) and copositive for 5-HTR2B (**Figure 1C**). The immunolabeled cells resemble smooth muscle adjacent ANO1 and 5-HTR2B positive ICCs observed in the female urethra [29]. The presence of both serotonin positive neuroendocrine cells and 5-HTR2B positive

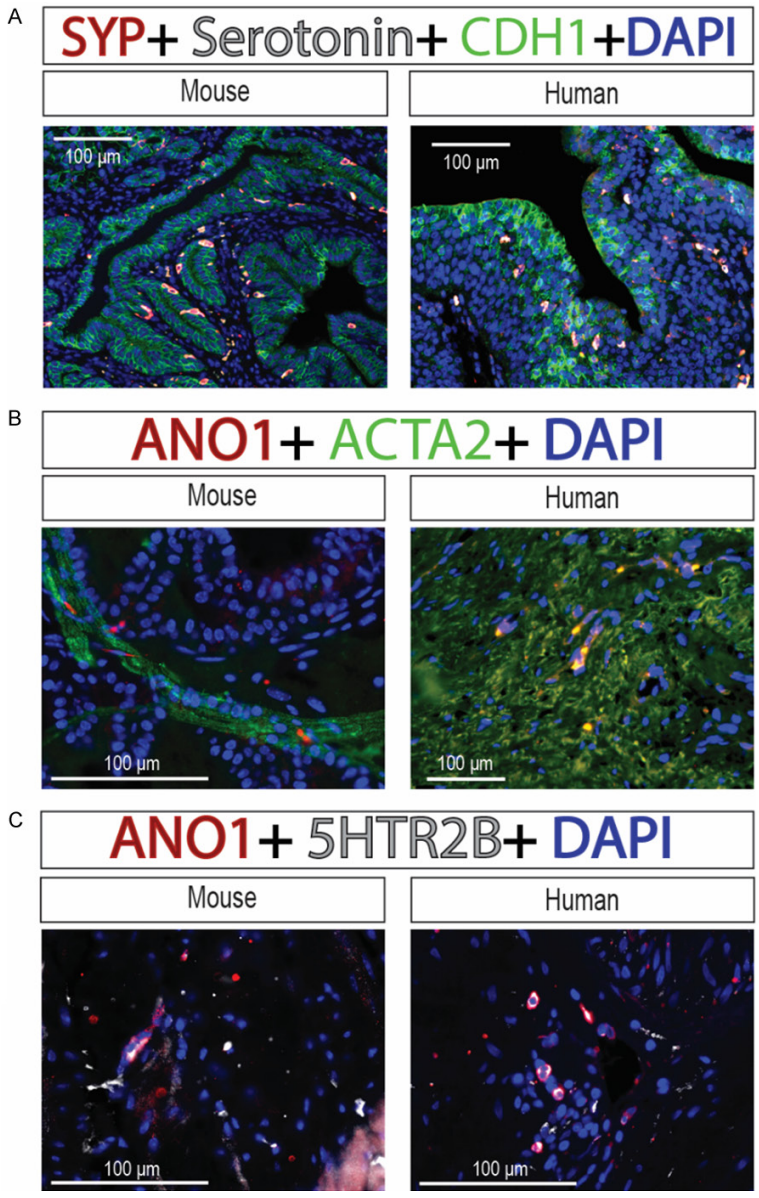

Figure 1. Serotonin producing neuroendocrine cells and serotonin receptor expressing, ANO1 positive Interstitial cells of Cajal are present in the prostate and urethra of adult male mice and humans. Immunofluorescent staining was performed on paraffin-embedded lower urinary tracts of 8-10-week-old male mice and on paraffin-embedded prostatic urethra tissue from human donors. (A) Synaptophysin (SYP, red), Serotonin (white), E-cadherin (CDH1, green) and 4',6-diamidino-2-phenylindole (DAPI, blue) were used to identify neuroendocrine cells at 20×. (B) Anoctamin-1 (ANO1, red) and actin alpha 2 (ACTA2, green) at 40× in mouse and 20x in human, and (C) ANO1 (red) and serotonin receptor 2b (HTR2B, white), and DAPI (blue) were used to identify interstitial cells of Cajal at 40×. Mouse images are representative of 3-6 individuals.

ICCs supports the hypothesis that the male prostatic urethra may generate serotonin induced contractions comparable to female urethra.

Exogenous T+E2 deteriorates spontaneous voiding behavior in wild type, but not Tph1$^{-/-}$ mice

To test if peripheral serotonin is necessary for T+E2 induced lower urinary tract dysfunction (LUTD) in male mice, we first established testing colonies of wild type and *Tph1*$^{-/-}$ mice. To collect a pre-surgery baseline, we used the void spot assay to compare spontaneous voiding behavior between genotype [15, 19]. There are no significant genotype differences for any measured metric of spontaneous voiding (total area, total number of spots, percent in corners, percent in center, number of any size spot). One to two days later, we performed sham surgery or placed sustained-release T+E2 implants into the scapular fat pad of mice from both genotypes. We repeated the void spot assay two weeks after sham or T+E2 implant surgery and performed a two way repeated measures ANOVA to compare VSA endpoints at baseline versus two weeks post implantation. In wild type mice, T+E2 treatment increases the number of urine spots, the total voided urine area, and the number of small spots (<0.01 mm) from genotype baseline (**Figure 2**). *Tph1*$^{-/-}$ mice are protected from these T+E2 mediated voiding changes, as none of the measured endpoints significantly differ from zero to two weeks in T+E2 treated, *Tph1*$^{-/-}$ mice (**Table 3**). A shift to smaller spots (0-0.1 cm) indicates lower urinary dysfunction leading to incomplete voids [14]. These results suggest that peripheral serotonin is responsible in part for T+E2-induced changes in spontaneous voiding behaviors of male mice.

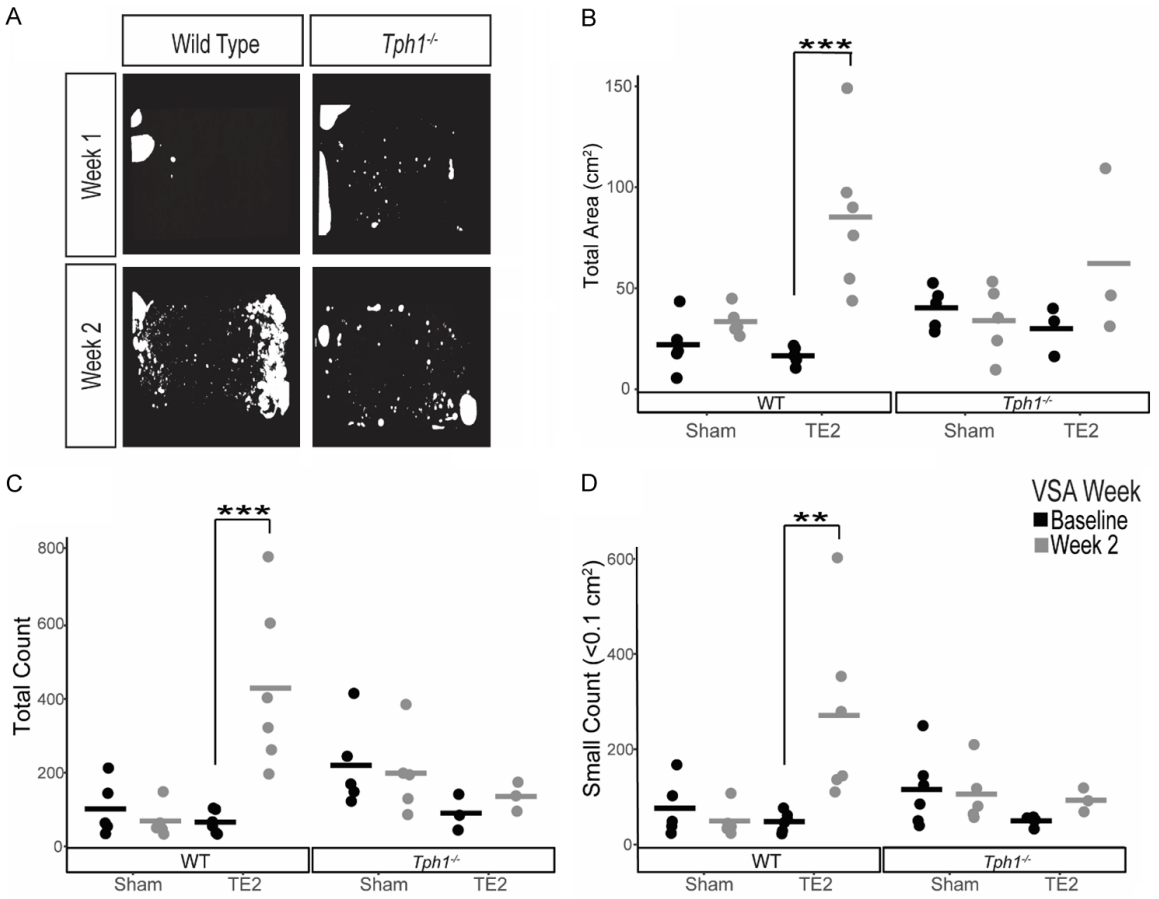

Figure 2. Exogenous T+E2 deteriorates voiding behavior in wild type, but not *Tph1*$^{-/-}$ mice. Void spot assays were conducted on mice one to two days before implantation of T+E2 or a sham pellet, and again two weeks post implantation. Representative images (A) show void spot papers from all treatment groups. Wild type mice treated with T+E2 exhibited sever voiding dysfunction after two weeks, with (B) increased total urine area, (C) total spot count, and (D) small spot count. Other treatment groups had no significant changes in voiding behavior. A two-way repeated ANOVA, followed by pairwise comparisons, was used to identify significant changes across time. *P*-values are represented by * and were calculated by Tukey's multiple comparisons test between baseline and week 2 within genotype and treatment group. *<0.05, **<0.01, ***<0.001.

Peripheral serotonin is required for T+E2-induced bladder underactivity, but not for T+E2 induced urinary retention in the bladder

T+E2 implants drive urinary retention in mice, characterized by incomplete bladder emptying and increased bladder volume [15, 41]. To evaluate whether peripheral serotonin contributes to this phenotype, four weeks after T+E2 implantation, mice were anesthetized, bladders were exteriorized, and dimensions were measured with a digital caliper along three axes to estimate volume. Bladder volumes were normalized to body weight to account for treatment/genotype-related differences in body size (**Figure 3A**). Relative bladder volume did not significantly differ between sham-treated wild type and *Tph1*$^{-/-}$ mice, indicating that peripheral serotonin deficiency alone does not affect baseline bladder volume. Bladder volume was significantly greater in T+E2-treated mice than in sham operated mice, regardless of genotype (**Figure 3B**).

To assess functional bladder outcomes, anesthetized cystometry was performed on male mice four weeks after T+E2 implantation (**Figure 4A** and **4B**). Six of seven T+E2-treated wild-type mice failed to generate a voiding contraction despite passive leakage of fluid from the urethral meatus, consistent with bladder underactivity. In contrast, only two of six T+E2 treated *Tph1*$^{-/-}$ mice failed to elicit a voiding contraction within the 1 hour monitoring period

Table 3. Exogenous testosterone and estradiol deteriorate spontaneous voiding behaviors in wild type, but not *Tph1*$^{-/-}$ mice

Void Spot Assay	Values are: Average							
	Wild Type				*Tph1*$^{-/-}$			
	Sham		T+E2		Sham		T+E2	
	Week 0 (Baseline)	Week 2	Week 0 (Baseline)	Week 2	Week 0 (Baseline)	Week 2	Week 0 (Baseline)	Week 2
Count	73.40	40.20	37.50	401.16***	191.6	170.40	61.67	107.33
Total Area (cm^2)	21.22	32.66	15.80	84.42***	39.49	33.14	29.15	61.53
Percent area in center	8.23	15.80	5.19	14.94	27.84	15.56	22.08	15.08
Percent area in corners	39.97	41.37	57.75	35.09	27.77	26.97	50.69	41.25
Spots of a certain size (cm^2)								
0-0.1	54.60	27.80	26.67	249.67**	93.83	84.00	27.75	71.33
4+	1.40	3.40	1.00	2.00	1.17	1.40	1.67	3.67

P-values are represented by * and were calculated by Tukey's multiple comparisons test between baseline and week 2 within genotype and treatment group. **<0.01, ***<0.001.

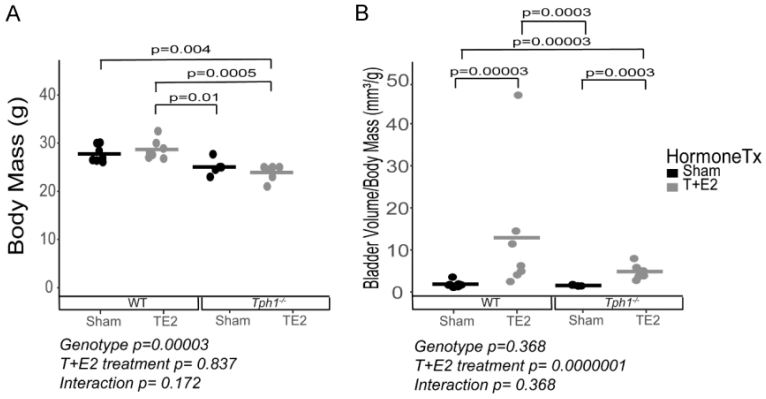

Figure 3. Peripheral serotonin is not required for testosterone and estradiol mediated urinary retention in male mice. Mice were treated as described in methods. Before cystometry, (A) mice were weighed and (B) bladders were externalized and measured with a digital caliper to calculate volume. Bladder volumes were then divided by overall body mass. Body masses and relative bladder volumes were compared using a two-way ANOVA followed by a Tukey's multiple comparisons test. Body masses were normalized using the reciprocal function when analyzed in A. Significant differences in body weights and bladder volumes are indicated with *p* values included on the graph. Solid lines indicate mean value; points represent individual mice.

(**Figure 4C**). These findings indicate that peripheral serotonin plays a role in T+E2-induced bladder underactivity.

Discussion

The current study confirmed the presence of serotonin-positive neuroendocrine cells and serotonin receptor-positive ICCs in the male human and mouse prostatic urethra (**Figure 1**), suggesting this region has the potential to produce serotonin induced contractions previously reported in female urethra [29]. We found that peripheral serotonin is at least in part required for T+E2 induced urinary voiding dysfunction in adult male mice. Specifically, peripheral serotonin is required for T+E2 induced small volume voiding, increased voiding frequency (**Table 3**), and bladder underactivity (**Figure 4**), as *Tph1*$^{-/-}$ mice retained baseline voiding behaviors and bladder activity. Urinary retention occurred regardless of genotype (**Figure 3**), indicating it is not serotonin dependent. The T+E2 induced urinary voiding dysfunction observed in wild type mice closely mirrors that reported by aging men: frequent small volume voids and incomplete bladder emptying. The progression of LUTD slowed in *Tph1*$^{-/-}$ mice, leading to a milder phenotype, indicating that serotonin could be an important target when considering treatment options to minimize LUTD. Reducing serotonin-induced contractions in symptomatic men could lead to improved voiding and quality of life without surgical intervention.

Anatomical and physiological responses to T+E2 in the current study resemble those described in previous studies [13-15, 24]. Long term exposure to T+E2 is known to cause bladder inactivity, as detrusor muscles become

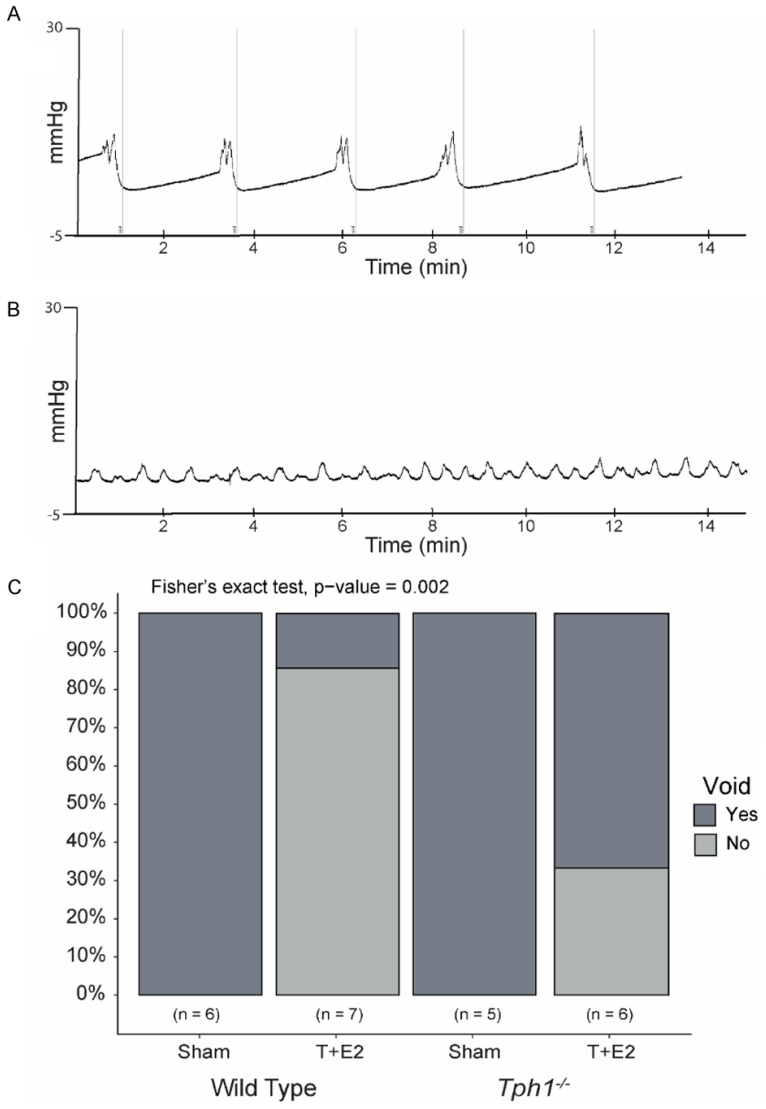

Figure 4. Peripheral serotonin is required for testosterone and estradiol mediated impairment of bladder contractility. Adult male wild type and *Tph1*$^{-/-}$ mice were then sham operated (control) or implanted with T+E2 pellets at 8-10 weeks of age. Mice were then anesthetized and evaluated by cystometry four weeks after implantation. Representative cystometry images show (A) successful voiding events, indicated by peaks in voiding pressure, in a wild type sham mouse and (B) no voiding events in a wild type T+E2 treated mouse. Cystometrograms include 15 minutes of the one-hour monitoring period. Vertical lines indicate the completion of a void. (C) Wild type T+E2 mice were significantly less likely to produce a successful voiding event, while *Tph1*$^{-/-}$ T+E2 mice retained the ability to void. A Fisher's exact test was used to calculate overall significance of genotype and treatment on cystometric outcomes.

overworked and fail [24]. Four months of exposure to exogenous T+E2 increases mouse prostate wet weight by 21%, mimicking the physical obstruction seen with BPH. The prostate invades the urethral lumen, and the luminal area detected from histological serial sections of euthanized mice is reduced to nearly half the size of sham operated control mice [15]. Estrogen is likely the key mediator of this growth, as removal of estrogen receptor alpha prevents LUTD [14]. Estrogen can also mediate serotonin production, reuptake, and receptor availability [42-44]. Because the *Tph1*$^{-/-}$ mice were protected from severe LUTD in the current study, future studies should examine the influence of 17β-estradiol on serotonin biosynthesis (*Tph1* abundance), serotonin reuptake (*Slc6a4* abundance), and serotonin receptor expression in the urethra.

Previous studies in female mice support a model in which inflammation stimulates serotonin release from neuroendocrine cells, activating urethral contractions. Lipopolysaccharide (LPS), a component of gram-negative bacterial cell walls, triggered urethral contractions ex vivo in a dose dependent manner, even in the presence of nerve blocking agents [29]. A similar model has been proposed in the lung and bowel, where serotonin controls smooth muscle contractions [45-47]. Together, these studies indicate that a trigger, like inflammation, causes the release of serotonin which initiates smooth muscle contractility, and that the severity of inflammation may dictate the degree of contraction. Inflammation is part of the sequalae of molecular and histological changes induced by T+E2 in mouse prostate and urethra and includes diffuse inflammation of all prostatic lobes characterized by the presence of macrophages and increased collagen fiber density [22, 23]. Although inflammatory proteins are significantly increased after as little

as three weeks of T+E2 treatment [17], inflammation does not peak until six weeks of T+E2 treatment [17, 22, 23]; two weeks after we completed the final cystometric measurements in T+E2 treated mice in the current study. Although the loss of peripheral serotonin synthesis protected against some T+E2 mediated endpoints, it did not protect against all of them. It would be useful for future studies to test if there is a similar requirement of peripheral serotonin in mouse models with more severe prostate inflammation than the T+E2 treated mouse.

Conclusion

This study indicates that serotonin plays a crucial role in the development of T+E2 induced LUTD. Mechanisms of male voiding dysfunction, particularly in the T+E2 treated model, have long been debated. A change in smooth muscle dynamics, mediated in part by serotonin secretion from neuroendocrine cells, may play a role. Further studies will need to investigate the triggers of these contractions and seek to identify potential serotonin mediated therapeutic targets for men who are impacted by LUTS.

Acknowledgements

This work was supported by NIH R25GM144-251, F31 ES036876, R01 ES035020, T32 ES007015, and U54 DK104309. The content is solely the responsibility of the authors and does not necessarily represent the official views of the National Institutes of Health.

Disclosure of conflict of interest

None.

Address correspondence to: Chad M Vezina, Department of Comparative Biosciences, University of Wisconsin-Madison, 2015 Linden Dr, Madison, WI 53706, United States. E-mail: chad.vezina@wisc.edu

References

[1] Kim EH, Larson JA and Andriole GL. Management of benign prostatic hyperplasia. Annu Rev Med 2016; 67: 137-151.

[2] Verhamme KM, Dieleman JP, Bleumink GS, van der Lei J, Sturkenboom MC, Artibani W, Begaud B, Berges R, Borkowski A, Chappel CR, Costello A, Dobronski P, Farmer RD, Jiménez Cruz F, Jonas U, MacRae K, Pientka L, Rutten FF, van Schayck CP, Speakman MJ, Sturkenboom MC, Tiellac P, Tubaro A, Vallencien G and Vela Navarrete R; Triumph Pan European Expert Panel. Incidence and prevalence of lower urinary tract symptoms suggestive of benign prostatic hyperplasia in primary care-the triumph project. Eur Urol 2002; 42: 323-328.

[3] Gasperi M, Krieger JN, Panizzon MS, Goldberg J, Buchwald D and Afari N. Genetic and environmental influences on urinary conditions in men: a classical twin study. Urology 2019; 129: 54-59.

[4] Partin AW, Page WF, Lee BR, Sanda MG, Miller RN and Walsh PC. Concordance rates for benign prostatic disease among twins suggest hereditary influence. Urology 1994; 44: 646-650.

[5] Eskenazi B, Warner M, Brambilla P, Signorini S, Ames J and Mocarelli P. The Seveso accident: A look at 40 years of health research and beyond. Environ Int 2018; 121: 71-84.

[6] Schenk JM, Kristal AR, Neuhouser ML, Tangen CM, White E, Lin DW, Kratz M and Thompson IM. Biomarkers of systemic inflammation and risk of incident, symptomatic benign prostatic hyperplasia: results from the prostate cancer prevention trial. Am J Epidemiol 2010; 171: 571-582.

[7] St Sauver JL and Jacobsen SJ. Inflammatory mechanisms associated with prostatic inflammation and lower urinary tract symptoms. Curr Prostate Rep 2008; 6: 67-73.

[8] Cohn JA. Urodynamics in the evaluation and management of bothersome lower urinary tract symptoms in men with a prostate. Neurourol Urodyn 2026; 45: 262-269.

[9] Ridlon M, Tlapa J and Stietz KK. Smooth muscle of the lower urinary tract: BK-RyR coupling in physiology and pathophysiology. J Muscle Res Cell Motil 2025; 46: 487-505.

[10] Harman SM, Metter EJ, Tobin JD, Pearson J and Blackman MR; Baltimore Longitudinal Study of Aging. Longitudinal effects of aging on serum total and free testosterone levels in healthy men. Baltimore longitudinal study of aging. J Clin Endocrinol Metab 2001; 86: 724-731.

[11] Golchin-Rad K, Mogheiseh A, Nazifi S, Ahrari Khafi MS, Derakhshandeh N and Abbaszadeh-Hasiri M. Changes in specific serum biomarkers during the induction of prostatic hyperplasia in dogs. BMC Vet Res 2019; 15: 440.

[12] Xu D, Wu Y, Shen H, Qian S and Qi J. High serum concentration of estradiol may be a risk factor of prostate enlargement in aging male in China. Aging Male 2020; 23: 1-6.

[13] Wynder JL, Nicholson TM, DeFranco DB and Ricke WA. Estrogens and male lower urinary tract dysfunction. Curr Urol Rep 2015; 16: 61.

[14] Nicholson TM, Moses MA, Uchtmann KS, Keil KP, Bjorling DE, Vezina CM, Wood RW and Ricke WA. Estrogen receptor-α is a key mediator and therapeutic target for bladder complications of benign prostatic hyperplasia. J Urol 2015; 193: 722-729.

[15] Nicholson TM, Ricke EA, Marker PC, Miano JM, Mayer RD, Timms BG, vom Saal FS, Wood RW and Ricke WA. Testosterone and 17β-estradiol induce glandular prostatic growth, bladder outlet obstruction, and voiding dysfunction in male mice. Endocrinology 2012; 153: 5556-5565.

[16] Bernoulli J, Yatkin E, Konkol Y, Talvitie EM, Santti R and Streng T. Prostatic inflammation and obstructive voiding in the adult noble rat: impact of the testosterone to estradiol ratio in serum. Prostate 2008; 68: 1296-1306.

[17] Bernoulli J, Yatkin E, Talvitie EM, Santti R and Streng T. Urodynamic changes in a noble rat model for nonbacterial prostatic inflammation. Prostate 2007; 67: 888-899.

[18] Trachtenberg J, Hicks LL and Walsh PC. Androgen- and estrogen-receptor content in spontaneous and experimentally induced canine prostatic hyperplasia. J Clin Invest 1980; 65: 1051-1059.

[19] Ruetten H, Wegner KA, Zhang HL, Wang P, Sandhu J, Sandhu S, Mueller B, Wang Z, Macoska J, Peterson RE, Bjorling DE, Ricke WA, Marker PC and Vezina CM. Impact of sex, androgens, and prostate size on C57BL/6J mouse urinary physiology: functional assessment. Am J Physiol Renal Physiol 2019; 317: F996-F1009.

[20] Tang XH, Liu ZY, Ren JW, Zhang H, Tian Y, Hu JX, Sun ZL and Luo GH. Comprehensive RNA-seq analysis of benign prostatic hyperplasia (BPH) in rats exposed to testosterone and estradiol. Sci Rep 2025; 15: 2750.

[21] Suzuki K, Ito K, Suzuki T, Honma S and Yamanaka H. Synergistic effects of estrogen and androgen on the prostate: effects of estrogen on androgen- and estrogen-receptors, BrdU uptake, immunohistochemical study of AR, and responses to antiandrogens. Prostate 1995; 26: 151-163.

[22] Popovics P, Silver SV, Uchtmann KS, Arendt LM, Vezina CM and Ricke WA. CCR2+ monocytes/macrophages drive steroid hormone imbalance-related prostatic fibrosis. Sci Rep 2024; 14: 15736.

[23] Popovics P, Skalitzky KO, Schroeder E, Jain A, Silver SV, Van Fritz F, Uchtmann KS, Vezina CM and Ricke WA. Steroid hormone imbalance drives macrophage infiltration and Spp1/osteopontin+ foam cell differentiation in the prostate. J Pathol 2023; 260: 177-189.

[24] Keil KP, Abler LL, Altmann HM, Wang Z, Wang P, Ricke WA, Bjorling DE and Vezina CM. Impact of a folic acid-enriched diet on urinary tract function in mice treated with testosterone and estradiol. Am J Physiol Renal Physiol 2015; 308: F1431-F1443.

[25] Wegner KA, Ruetten H, Girardi NM, O'Driscoll CA, Sandhu JK, Turco AE, Abler LL, Wang P, Wang Z, Bjorling DE, Malinowski R, Peterson RE, Strand DW, Marker PC and Vezina CM. Genetic background but not prostatic epithelial beta-catenin influences susceptibility of male mice to testosterone and estradiol-induced urinary dysfunction. Am J Clin Exp Urol 2021; 9: 121-131.

[26] Chavalmane AK, Comeglio P, Morelli A, Filippi S, Fibbi B, Vignozzi L, Sarchielli E, Marchetta M, Failli P, Sandner P, Saad F, Gacci M, Vannelli GB and Maggi M. Sex steroid receptors in male human bladder: expression and biological function. J Sex Med 2010; 7: 2698-2713.

[27] Nguyen ST, Prakash R, Anderson CJ, Frydenberg M and Haynes JM. Sex steroids modulate α1-adrenoceptor-stimulated Ca2+ elevation in human cultured prostatic stromal cells. Prostate 2007; 67: 74-82.

[28] Cha JY, Wee J, Jung J, Jang Y, Lee B, Hong GS, Chang BC, Choi YL, Shin YK, Min HY, Lee HY, Na TY, Lee MO and Oh U. Anoctamin 1 (TMEM16A) is essential for testosterone-induced prostate hyperplasia. Proc Natl Acad Sci U S A 2015; 112: 9722-9727.

[29] Ambrogi M, Hernandez LL, Strand DW, Kumar S, Romero MF, Barasch J, Ridlon M, Keil Stietz KP and Vezina CM. A 5-HT-mediated urethral defense against urinary tract infections. Proc Natl Acad Sci U S A 2025; 122: e2409754122.

[30] Sanders KM, Ward SM and Koh SD. Interstitial cells: regulators of smooth muscle function. Physiol Rev 2014; 94: 859-907.

[31] Mehta V, Abler LL, Keil KP, Schmitz CT, Joshi PS and Vezina CM. Atlas of Wnt and R-spondin gene expression in the developing male mouse lower urogenital tract. Dev Dyn 2011; 240: 2548-2560.

[32] Instructional Video: Overview of embedding prostatic urethra in transverse plane | ATLAS-D2K. https://www.atlas-d2k.org/chaise/record/#2/Common:Instructional_Video/RID=16-QSGY.

[33] Ruetten H, Sandhu SK, Fox O, Zhu J, Sandhu JK and Vezina CM. The impact of short term, long term and intermittent E. coli infection on male C57BL/6J mouse prostate histology and urinary physiology. Am J Clin Exp Urol 2023; 11: 59-68.

[34] Nebigil CG, Choi DS, Dierich A, Hickel P, Le Meur M, Messaddeq N, Launay JM and Maroteaux L. Serotonin 2B receptor is required for heart development. Proc Natl Acad Sci U S A 2000; 97: 9508-9513.

[35] Saini S, Sreekumar A, Nathani S, Asante DM and Simmons MN. A novel exosome based therapeutic intervention against neuroendocrine prostate cancer. Sci Rep 2024; 14: 2816.
[36] Hill WG, Zeidel ML, Bjorling DE and Vezina CM. Void spot assay: recommendations on the use of a simple micturition assay for mice. Am J Physiol Renal Physiol 2018; 315: F1422-F1429.
[37] Wegner KA, Abler LL, Oakes SR, Mehta GS, Ritter KE, Hill WG, Zwaans BM, Lamb LE, Wang Z, Bjorling DE, Ricke WA, Macoska J, Marker PC, Southard-Smith EM, Eliceiri KW and Vezina CM. Void spot assay procedural optimization and software for rapid and objective quantification of rodent voiding function, including overlapping urine spots. Am J Physiol Renal Physiol 2018; 315: F1067-F1080.
[38] Lee SH, Lysiak JJ and Steers WD. Bladder and urethral function in a mouse model of cavernous nerve injury. Neurourol Urodyn 2013; 32: 1038-1043.
[39] Uemura KI, Hiroshige T, Ueda K, Ohta K, Hayashi T, Hirashima S, Kanazawa T, Nakiri M, Igawa T and Nakamura KI. Distribution, shape, and immunohistochemical characteristics of serotonin-immunoreactive neuroendocrine cells in the urethra and periurethral genital organs in mice. J Mol Histol 2021; 52: 1205-1214.
[40] Acosta S, Dizeyi N, Pierzynowski S, Alm P and Abrahamsson PA. Neuroendocrine cells and nerves in the prostate of the guinea pig: effects of peripheral denervation and castration. Prostate 2001; 46: 191-199.
[41] Ricke WA, Lee CW, Clapper TR, Schneider AJ, Moore RW, Keil KP, Abler LL, Wynder JL, López Alvarado A, Beaubrun I, Vo J, Bauman TM, Ricke EA, Peterson RE and Vezina CM. In utero and lactational TCDD exposure increases susceptibility to lower urinary tract dysfunction in adulthood. Toxicol Sci 2016; 150: 429-440.
[42] Moses-Kolko EL, Berga SL, Greer PJ, Smith G, Cidis Meltzer C and Drevets WC. Widespread increases of cortical serotonin type 2A receptor availability after hormone therapy in euthymic postmenopausal women. Fertil Steril 2003; 80: 554-559.
[43] Kugaya A, Epperson CN, Zoghbi S, van Dyck CH, Hou Y, Fujita M, Staley JK, Garg PK, Seibyl JP and Innis RB. Increase in prefrontal cortex serotonin 2A receptors following estrogen treatment in postmenopausal women. Am J Psychiatry 2003; 160: 1522-1524.
[44] Hudon Thibeault AA, Sanderson JT and Vaillancourt C. Serotonin-estrogen interactions: what can we learn from pregnancy? Biochimie 2019; 161: 88-108.
[45] Yu Y, Yang W, Li Y and Cong Y. Enteroendocrine cells: sensing gut microbiota and regulating inflammatory bowel diseases. Inflamm Bowel Dis 2020; 26: 11-20.
[46] Noguchi M, Furukawa KT and Morimoto M. Pulmonary neuroendocrine cells: physiology, tissue homeostasis and disease. Dis Model Mech 2020; 13: dmm046920.
[47] Huang X, Choi S, Wu W, Shahi PK, Lee JH, Hong C and Jun JY. 5-hydroxytryptamine enhances the pacemaker activity of interstitial cells of cajal in mouse colon. Int J Mol Sci 2024; 25: 3997.